International Journal of Chemical and Biochemical Sciences
(ISSN 2226-9614)

Journal Home page: www.iscientific.org/Journal.html

Computational Analysis of Irregularity Measures of Molecular Structure of Copper Oxide

Asfand Yar Khan[1], *Muhammad Haroon Aftab*[1*], *Ali Haidar*[1]

[1]*Department of Mathematics and Statistics, The University of Lahore, Lahore 54500, Pakistan*

Abstract

The crystallographic structure of copper [I] oxide is an irregular graph, so degree of vertex of some vertices is different. Irregularity indices of copper [I] oxide play an important role to understand the significance and properties of structure of copper [I] oxide and gain attention of researchers. In this study, we are interested to deal with irregularity indices for copper [I] oxide. This study explores the application of irregularity indices derived from graph theory to analyze the crystal structure of copper [I] oxide Cu_2O [m; n]. We also construct table for edge partition of Cu_2O [m; n]. This study is not only advancing our understanding of the crystallographic irregularities in Cu_2O [m; n] but also demonstrates the utility of graph-based irregularity indices in the study of Cu_2O [m; n]. From this work, we analyzed the relationship between irregularity indices and physicochemical properties like boiling point, enthalpy of copper [I] oxide. The outcomes of this investigation have broader implications for the field of chemical graph, providing a foundation for future research on quantitative structure property relationships. In this work, crystallographic structure of Cu_2O [m; n], irregularity measures (IMs), computation of edge partition of Cu_2O [m; n], computation of irregularity indices for Cu_2O [m; n], computation of physicochemical properties such as boiling point, enthalpy, molar volume and molar mass of copper [I] oxide have been discussed.

Keywords: Topological indices; Irregularity indices; copper oxide; vertex; edge.

Full-length article **Corresponding Author*, e-mail: haroonuet@gmail.com Doi # https://doi.org/10.62877/124-IJCBS-24-25-19-124

1. Introduction

Graph theory is a branch of discrete mathematics that deals with the study of graphs, which are mathematical structures used to model pairwise relationships between objects. The basics of graph theory are vertices and edges that are fundamental units of graph. Vertices are points or nodes in the graph and edges are connections or links among vertices in the graph [1]. In chemical graph theory, a molecular graph, which also called chemical graph, is a representation of the structural formula of a chemical compound in terms of graph theory. In graph, there are some vertices, edges so in chemical graph vertices correspond to the atoms of the chemical compound and edges correspond to the chemical bonds between the elements [2]. Copper is a chemical element with the symbol Cu and atomic number 29. It is a soft, malleable and ductile metal with very high thermal and electrical conductivity. Copper exhibits a rich coordination chemistry with complexes known in oxidation states ranging from 0 to +4, although the +2 (cupric) and the +1 (cuprous) oxidation states are by far the most common, with +2 predominating.

Compounds of copper have found extensive practical usage, including as catalysts in both homogeneous and heterogeneous reactions, as fungicides, pesticides, and wood preservatives, as pigments for paints and glasses, and in the so-called high-temperature superconductors. Copper oxide is a compound, which formed due to oxygen and copper. Copper oxide has many forms. They form when oxygen combines with copper in different ways. The most common form of copper oxide is copper [I] oxide [3]. In Cu_2O [m; n], m represents the number of unit cells in row and n represents the number of unit cells in column. If there is one-unit cell in row and one- unit cell in column, then we write copper [I] oxide Cu_2O [1; 1]. If there are two-unit cells in row and two-unit cells in column then we write copper [I] oxide Cu_2O [2; 2] as well and if there are four-unit cells in row and also four-unit cells in column then we write copper [I] oxide Cu_2O [4; 4], respectively. Copper [I] oxide or cuprous oxide is an inorganic compound also called di-copper oxide or red copper oxide with the chemical formula Cu_2O [m; n]. It is covalent in nature. Cu_2O [m; n] crystallizes in a cubic structure.

It has reddish black or reddish-brown appearance. It is p-type semiconductor material. Its melting point is very high which is 1232°C and its boiling point is 1800°C. Copper [I] oxide is insoluble in water and soluble in concentrated ammonia solution and slightly soluble in dilute acids. It does not show any significant magnetic properties. It has low thermal conductivity as compared to copper. Copper [I] oxide is used in the production of solar cell [4], use as a pigment in ceramics and in certain electronic devices also. It used in the production of photo detectors that detect light and convert it

into an electrical signal [5]. Cu_2O [m; n] is a semiconductor with a direct band gap, making it suitable for applications in electronic devices [6]. It has studied for its potential use in the fabrication of field effect transistors and other semiconductor components [7]. The photo catalytic properties of Cu_2O [m; n] make it useful in environmental applications. It has been explored for the degradation of organic pollutants and the reduction of carbon dioxide through photo catalytic reactions [8], contributing to sustainable energy and environmental technologies. Cu_2O [m; n] has demonstrated sensitivity to various gases, such as carbon monoxide and ammonia. This property makes it applicable in gas sensors for monitoring air quality and detecting harmful gases [9].

Due to its antimicrobial properties, Cu_2O [m; n] has been considered for use in antifouling coatings. These coatings help prevent the growth of marine organisms on ship hulls, reducing drag and improving fuel efficiency [10]. Copper [I] oxide has been investigated for its potential as a high temperature superconductor, which could have applications in various industries, including energy transmission and medical imaging. Cu_2O [m; n] has been studied for its use in battery electrodes, contributing to the development of next-generation batteries with improved energy storage capacity [11]. Copper [I] oxide serves as a catalyst in organic synthesis, promoting various chemical reactions [12]. It has applications in the production of fine chemicals and pharmaceuticals [13]. The unique properties of Cu_2O nanoparticles make them attractive for applications in nanotechnology, including drug delivery [14-15], imaging and sensing. In the realm of electronics, it serves as a photovoltaic cell material due to its potential as a semiconductor [16]. Its fungicidal and bactericidal properties make it a vital component in the production of antifouling paints, used to prevent the growth of marine organisms on ship nulls [17-18]. It employed as a catalyst for variety of chemical reactions, including the decomposition of carbon monoxide and the synthesis of methanol [19].

It is utilized an electrode material in lithium-ion batteries and other energy storage systems due to its high theoretical capacity [20]. A topological index is a type of molecular descriptor which is a numerical value associated with a graph that captures certain structural properties of the molecular graph and describes topology of graph, analyze mathematical values and further investigate some physicochemical properties of a molecule. Some most significant types of topological indices are distance based, degree based and spectrum based topological indices [21]. These indices provide insights into various physicochemical properties, such as molecular size, shape, stability, and biological activity, without needing to know the specific atomic coordinates or detailed electronic structure of the molecule. They are particularly useful for high-throughput screening and virtual screening in drug discovery, as well as in quantitative structure-activity relationship (QSAR) studies. Quantitative structure-activity relationship (QSAR) is a computational technique used to predict the biological activity, toxicity, or other properties of chemical compounds based on their molecular structure [22]. Topological indices often used as molecular descriptors in QSAR studies to correlate chemical structure with biological activity [23]. In the pharmaceutical industry, topological indices used in virtual screening and drug design to identify potential drug candidates with desired properties.

Topological indices can used to predict various physicochemical properties of chemical compounds, such as boiling point, melting point, solubility, and partition coefficient. Topological indices employed to measure the similarity between chemical compounds or to cluster compounds based on structural similarity. This is useful in drug discovery, environmental chemistry, and toxicology. Topological indices used in teaching and research to analyze the structure-property relationships of chemical compounds and to develop new computational methods for molecular modeling and simulation. An irregularity index is a statistical value connected with a graph that measures the irregularity of graph. The irregularity index measures how much the degrees of vertices deviate from the average degree. A lower irregularity index indicates a more regular or balanced distribution of degrees, while a higher irregularity index suggests a more irregular or unbalanced distribution. A graph G is a regular if degree of all vertices is same otherwise it is called irregular [24]. His first Zagreb index [25] and the second Zagreb index [26] of a graph G denoted by M_1 and M_2 respectively and defined as

$$M_1(G) = \sum_{uv \in E(G)} (d_u + d_v),$$

$$M_2(G) = \sum_{uv \in E(G)} (d_u \, . \, d_v).$$

The modification of first Zagreb index denoted by F (G), which called forgotten index [27] and defined as

$$F(G) = \sum_{uv \in E(G)} (d_u^2 + d_v^2).$$

The Albertson index [28] which is also called third Zagreb index is denoted by Al (G) or IRR (G) and defined as

$$IRR(G) = \sum_{pq \in E(G)} |d_p - d_q|.$$

The Bell's degree variance is one of the most popular degree-based irregularity indices which is denoted by VAR (G) [29] and defined as

$$VAR(G) = \sum_{pq \in E(G)} \frac{M_1(G)}{s} - \left(\frac{2r}{s}\right)^2.$$

The sigma index [30] is an important degree based topological index, which denoted by IRF (G) or σ (G) and formulated as

$$IRF(G) = \sum_{pq \in E(G)} (d_p - d_q)^2.$$

Irregularity indices provide quantitative measures of the structural complexity of graphs. In chemistry, molecular graphs represent chemical compounds, and irregularity indices help quantify the complexity of their molecular structures. This complexity can related to various physicochemical properties or biological activities of the molecules. Irregularity indices allow for the differentiation between different molecular structures based on their topological features. By calculating irregularity indices for molecular graphs, chemists can compare and classify molecules according to their structural complexity. This is crucial in various fields such as drug design, where structurally diverse compounds need to evaluate for their potential biological activities. Irregularity indices can correlated with various properties or activities of molecules. By analyzing the relationship between irregularity indices and experimental data, such as biological activity or toxicity,

researchers can gain insights into the structure-activity relationships of chemical compounds. This information is valuable for predicting the properties of new compounds and optimizing their design.

2. Preliminaries

Graph theory as a formal mathematical discipline not invented by a single individual but rather evolved over time through the contributions of many mathematicians. However, one of the key Figures credited with laying the foundation of graph theory is Leonhard Euler, and 18th century Swiss mathematician. In 1736, Euler published a paper titled "Solutio problematis and geometriam situs pertinentis" (Solution of a problem relating to the geometry of position), which is considered the starting point of graph theory. In this paper, Euler addressed the famous Seven Bridges of Konigsberg problem, which involved determining whether it was possible to walk through the city of Konigsberg and cross each of its seven bridges exactly once, returning to the starting point. Euler abstracted the problem to represent the landmasses as vertices and the bridges as edges, thus creating a mathematical structure that we now recognize as a graph. By analyzing the properties of this graph, Euler was able to prove that it was not possible to traverse all bridges exactly once, laying the foundation for the study of graphs and networks emerge until the 18th century. However, some precursor works laid the foundation for later developments.

Leonhard Euler (1707-1783): Euler often considered the father of graph theory. In 1736, he solved the famous Seven Bridges of Konigsberg problem, which considered one of the first problems in graph theory. Euler's solution did not use the language of graphs as we know it today, but his method of abstracting the problem into a graph laid the groundwork for the formalization of graph theory [31]. Daniel Bernoulli (1700-1782): Euler's colleague Daniel Bernoulli also contributed to early graph theory. He introduced the concept of the network in his work on the "brachistochrone" problem, which deals with finding the curve between two points in which a body acted upon only by gravity will move along the shortest path [32]. Eulerian paths: Euler's work on the Seven Bridges problem led to the concepts of Eulerian paths and circuits. An Eulerian path is a path in a graph that visits every edge exactly once, while an Eulerian circuit is a closed path that visits every edge exactly once [33].

The 19th century saw further development and refinement of graph theory concepts, building upon the foundation laid in the 18th century. Gustav Kirchhoff (1824-1887): Kirchhoff, a German physicist, made significant contributions to the application of graph theory in electrical circuit analysis. His work on the laws governing electrical circuits, known as Kirchhoff's laws, involved representing electrical networks as graphs. He introduced the concept of a graph's "tree" in this context, which later became important in the study of spanning trees [34]. Topological Indices: Topological indices [35-41] used on chemical graphs for several reasons, primarily to quantify and analyze the structural properties of molecules. These indices provide numerical descriptors that capture certain topological features of molecular graphs, which in turn can correlated with various physical, chemical, and biological properties of molecules.

3. Materials and Methods

3.1. Materials

We needed some crystallographic structure and other relevant information for copper [I] oxide. We use following specific irregularity indices on chemical graph of copper [I] oxide. Let G_1 and G_2 be two graphs of copper [I] oxide, respectively. In Cu_2O [m; n], m represents the number of unit cells in row and n represents the number of unit cells in column. The terms r and s define the number of edges and number of vertices respectively. Here for G_1, $r = 8mn$ & $s = 7mn + 2m + 2n + 2$ and for G_2, $r = 12mn$ & $s = 8mn + 2m + 2n$.

$$IRDIF(G) = \sum_{pq \in E(G)} \left|\frac{d_p}{d_q} - \frac{d_q}{d_p}\right|, \quad (1)$$

$$IRR(G) = \sum_{pq \in E(G)} |d_p - d_q|, \quad (2)$$

$$IRL(G) = \sum_{pq \in E(G)} |\ln d_p - \ln d_q|, \quad (3)$$

$$IRLF(G) = \sum_{pq \in E(G)} \frac{|d_p - d_q|}{\sqrt{d_p . d_q}}, \quad (4)$$

$$IRF(G) = \sum_{pq \in E(G)} (d_p - d_q)^2, \quad (5)$$

$$IRA(G) = \sum_{pq \in E(G)} \left(d_p^{-½} - d_q^{-½}\right)^2, \quad (6)$$

$$IRB(G) = \sum_{pq \in E(G)} \left(\sqrt{d_p} - \sqrt{d_q}\right)^2, \quad (7)$$

$$IRLA(G) = \sum_{pq \in E(G)} 2\left(\frac{|d_p - d_q|}{(d_p + d_q)}\right), \quad (8)$$

$$IRLD_1(G) = \sum_{pq \in E(G)} \ln\{1 + |d_p - d_q|\}, \quad (9)$$

$$IRGA(G) = \sum_{pq \in E(G)} \ln\frac{(d_p + d_q)}{2\sqrt{d_p . d_q}}, \quad (10)$$

$$VAR(G) = \sum_{pq \in E(G)} \frac{M_1(G)}{s} - \left(\frac{2r}{s}\right)^2, \quad (11)$$

$$IR1(G) = F(G) - \frac{2r}{s} M_1(G), \quad (12)$$

$$IR2(G) = \sqrt{\frac{M_2(G)}{r}} - \frac{2r}{s}, \quad (13)$$

$$IRFW(G) = \frac{IRF(G)}{M_2(G)}, \quad (14)$$

$$IRC(G) = \sum_{pq \in E(G)} \left(\frac{\sqrt{d_p . d_q}}{r} - \frac{2r}{s}\right), \quad (15)$$

$$M_1(G) = \sum_{uv \in E(G)} (d_u + d_v), \quad (16)$$

$$M_2(G) = \sum_{uv \in E(G)} (d_u . d_v), \quad (17)$$

$$F(G) = \sum_{uv \in E(G)} (d_u^2 + d_v^2). \quad (18)$$

3.2. Methods

3.2.1. Edge partition of $G_1 \approx Cu_2O$ [m; n]

There are three partitions of edges in Cu_2O [m; n] on the base of degree. We computed number of indices for each

number of edges. $E_{(d_p,d_q)}$ Shows the number of edges bounded by the vertices having degrees d_p and d_q, respectively and shown in Table 1. Different dimensional structures of copper [I] oxide are depicted in Figure 1-3.

$$E_{(1,2)} = \{e = pq \in E(G) | d_p = 1;\ d_q = 2\},$$
$$E_{(2,2)} = \{e = pq \in E(G) | d_p = 2;\ d_q = 2\},$$
$$E_{(2,4)} = \{e = pq \in E(G) | d_p = 2;\ d_q = 4\}.$$

4. Main Results

4.1. Computation of irregularity indices for copper [I] oxide $G_1 \approx Cu_2O$ [m; n]

Theorem 1: *Let G be a graph of copper [I] oxide then its irregularity index IRDIF computed as*

Proof: We know that,

$$IRDIF(G_1) = \sum_{pq\in E}\left|\frac{d_p}{d_q} - \frac{d_q}{d_p}\right|.$$

$$IRDIF(Cu_2O[m;\ n]) = (4m+4n-4)\left|\frac{1}{2}-\frac{2}{1}\right| + (4mn-4m-4n+4)\left|\frac{2}{2}-\frac{2}{2}\right| + (4mn)\left|\frac{2}{4}-\frac{4}{2}\right|$$
$$= (4m+4n-4)\left|-\frac{3}{2}\right| + (4mn-4m-4n+4)|0| + (4mn)\left|-\frac{3}{2}\right|.$$
$$= \frac{3}{2}(4m+4n-4) + \frac{3}{2}(4mn) = 6m+6n-6+6mn.$$
$$\Rightarrow IRDIF(Cu_2O[m;\ n]) = 6mn+6m+6n-6.$$

Theorem 2: *Let G be a graph of copper [I] oxide then its irregularity index IRR computed as*

Proof: We know that,

$$IRR(G_1) = \sum_{pq\in E}|d_p - d_q|.$$
$$IRR(Cu_2O[m;\ n]) = (4m+4n-4)|1-2| + (4mn-4m-4n+4)|2-2| + (4mn)|2-4|$$
$$= (4m+4n-4)|-1| + (4mn-4m-4n+4)|0| + (4mn)|-2|.$$
$$\Rightarrow IRR(Cu_2O[m;\ n]) = 8mn+4m+4n-4.$$

Theorem 3: *Let G be a graph of copper [I] oxide then its irregularity index IRL computed as*

Proof: We know that,

$$IRL(G_1) = \sum_{pq\in E}|\ln d_p - \ln d_q|.$$
$$IRL(Cu_2O[m;\ n]) = (4m+4n-4)|\ln 2 - \ln 1| + (4mn-4m-4n+4)|\ln 2 - \ln 2| + (4mn)|\ln 4 - \ln 2|.$$
$$= (4m+4n-4)|\ln 2| + (4mn-4m-4n+4)|0| + (4mn)|\ln 2|.$$
$$= (4m+4n-4)|\ln 2| + (4mn)|\ln 2|.$$
$$\Rightarrow IRL(Cu_2O[m;\ n]) = (4mn+4m+4n-4)|\ln 2|.$$

Theorem 4: *Let G be a graph of copper [I] oxide then its irregularity index IRLF computed as*

Proof: We know that,

$$IRLF(G_1) = \sum_{pq\in E}\frac{|d_p-d_q|}{\sqrt{(d_p.d_q)}}.$$

$$IRLF(Cu_2O[m;\ n]) = (4m+4n-4)\frac{|2-1|}{\sqrt{2}} + (4mn-4m-4n+4)\frac{|2-2|}{\sqrt{4}} + (4mn)\frac{|4-2|}{\sqrt{8}} = (4m+4n-4)\frac{1}{\sqrt{2}} + (4mn)\frac{2}{2\sqrt{2}}.$$
$$\Rightarrow IRLF(Cu_2O[m;\ n]) = (4mn+4m+4n-4)\frac{1}{\sqrt{2}}.$$

Theorem 5: *Let G be a graph of copper [I] oxide then its irregularity index IRF computed as*

Proof: We know that,

$$IRF(G_1) = \sum_{pq\in E}(d_p - d_q)^2.$$
$$IRF(Cu_2O[m;\ n]) = (4m+4n-4)(2-1)^2 + (4mn-4m-4n+4)(2-2)^2 + 4mn(4-2)^2 = 4m+4n-4+4mn(2)^2.$$
$$\Rightarrow IRF(Cu_2O[m;\ n]) = 16mn+4m+4n-4.$$

Theorem 6: *Let G be a graph of copper [I] oxide then its irregularity index IRA computed as*

Proof: We know that,

$$IRA(G_1) = \sum_{pq\in E}\left(d_p^{-\frac{1}{2}} - d_q^{-\frac{1}{2}}\right)^2.$$

$$IRA(Cu_2O[m;\ n]) = (4m+4n-4)\left(\frac{1}{\sqrt{2}}-\frac{1}{\sqrt{1}}\right)^2 + (4mn-4m-4n+4) + (4mn)\left(\frac{1}{\sqrt{4}}-\frac{1}{\sqrt{2}}\right)^2$$
$$= (4m+4n-4)\left(\frac{1-\sqrt{2}}{\sqrt{2}}\right)^2 + (4mn)\left(\frac{1-\sqrt{2}}{2}\right)^2.$$
$$= (4m+4n-4)\frac{(1-\sqrt{2})^2}{2} + (4mn)\frac{(1-\sqrt{2})^2}{4}$$
$$= (2mn+4m+4n-4)\frac{(1-\sqrt{2})^2}{2}.$$
$$\Rightarrow IRA(Cu_2O[m;\ n]) = (mn+2m+2n-2)\left(1-\sqrt{2}\right)^2.$$

Theorem 7: *Let G be a graph of copper [I] oxide then its irregularity index IRB computed as*

Proof: We know that,

$$IRB(G_1) = \sum_{pq\in E}\left(\sqrt{d_p} - \sqrt{d_q}\right)^2.$$

$$IRB(Cu_2O[m;\ n]) = (4m+4n-4)\left(\sqrt{2}-\sqrt{1}\right)^2 + (4mn-4m-4n+4) + 4mn\left(\sqrt{4}-\sqrt{2}\right)^2$$
$$\left(\sqrt{2}-\sqrt{2}\right)^2 + 4mn\left(\sqrt{4}-\sqrt{2}\right)^2$$
$$= (4m+4n-4)\left(\sqrt{2}-1\right)^2 + 8mn\left(\sqrt{2}-1\right)^2.$$
$$\Rightarrow IRB(Cu_2O[m;\ n]) = (8mn+4m+4n-4)\left(\sqrt{2}-1\right)^2.$$

Theorem 8: *Let G be a graph of copper [I] oxide then its irregularity index IRLA computed as*

Proof: We know that,

$$IRLA(G_1) = \sum_{pq\in E} 2\frac{|d_p-d_q|}{(d_p+d_q)}.$$

$$IRLA(Cu_2O[m;\ n]) = 2(4m+4n-4)\frac{|2-1|}{(2+1)} + 2(4mn-4m-4n+4)\frac{|2-2|}{(2+2)} + 2(4mn)\frac{|4-2|}{(4+2)} =$$
$$(4m+4n-4)\frac{2}{3} + (8mn)\frac{2}{6}.$$
$$\Rightarrow IRLA(Cu_2O[m;\ n]) = \frac{2}{3}(4mn+4m+4n-4).$$

Theorem 9: *Let G be a graph of copper [I] oxide then its irregularity index $IRLD_1$ computed as*

Proof: We know that,

$$IRLD_1(G_1) = \sum_{pq\in E}\ln\{1+|d_p-d_q|\}.$$
$$IRLD_1(Cu_2O[m;\ n]) = (4m+4n-4)\ln\{1+|2-1|\} + (4mn-4m-4n+4)\ln\{1+|2-2|\} + (4mn)\ln\{1+|4-2|\}.$$
$$= (4m+4n-4)\ln 2 + (4mn-4m-4n+4)\ln 1 + (4mn)\ln\{1+2\}.$$
$$\Rightarrow IRLD_1(Cu_2O[m;\ n]) = (4m+4n-4)\ln 2 + (4mn)\ln 3.$$

Theorem 10: *Let G be a graph of copper [I] oxide then its irregularity index IRGA computed as*

Proof: We know that,

$\mathrm{IRGA}\ (G_1) = \sum_{pq\in E} \ln\left(\frac{(d_p+d_q)}{2\sqrt{d_p.d_q}}\right)$.

$\mathrm{IRGA}\ (Cu_2O\ [m;\ n]) = (4m+4n-4)\ln\left(\frac{1+2}{2\sqrt{2\ .\ 1}}\right) + (4mn-4m-4n+4)\ln\left(\frac{2+2}{2\sqrt{2\ .\ 2}}\right) + (4mn)\ln\left(\frac{2+4}{2\sqrt{2\ .4}}\right)$.

$= (4m+4n-4)\ln\frac{3}{2\sqrt{2}} + (4mn-4m-4n+4)\ln 1 + (4mn)\ln\frac{6}{4\sqrt{2}}$.

$\Rightarrow \mathrm{IRGA}\ (Cu_2O\ [m;\ n]) = (4mn+4m+4n-4)\ln\frac{3}{2\sqrt{2}}$.

Theorem 11: *Let G be a graph of copper [I] oxide then its irregularity index VAR computed as*

Proof: We know that,

$\mathrm{VAR}\ (G_1) = \frac{M_1(G)}{s} - \left(\frac{2r}{s}\right)^2$ & $M_1\ (G_1) = \sum_{pq\in E}(d_p+d_q)$.

$M_1\ (Cu_2O\ [m;\ n]) = (4m+4n-4)(1+2) + (4mn-4m-4n+4)(2+2) + 4mn(2+4)$

$= 3(4m+4n-4) + 4(4mn-4m-4n+4) + 6(4mn)$.

$= 12m+12n-12+16mn-16m-16n+16+24mn$.

$\Rightarrow M_1\ (Cu_2O\ [m;\ n]) = 40mn-4m-4n+4$.

$\mathrm{VAR}\ (Cu_2O\ [m;\ n]) = \frac{40mn-4m-4n+4}{s} - \left(\frac{2r}{s}\right)^2\frac{40mn-4m-4n+4}{s} - \left(\frac{4r^2}{s^2}\right)$.

$= \frac{40mn-4m-4n+4}{7mn+2m+2n+2} - \frac{4(8mn)}{(7mn+2m+2n+2)^2}$

$\frac{(7mn+2m+2n+2)(40mn-4m-4n+4)-4(64m^2n^2)}{(7mn+2m+2n+2)^2}$.

$= \frac{24m^2n^2+52m^2n+52mn^2+92mn-8m^2-8n^2+8}{(7mn+2m+2n+2)^2}$.

Theorem 12: *Let G be a graph of copper [I] oxide then its irregularity index IR1 computed as*

Proof: We know that,

$\mathrm{IR1}\ (G_1) = F\ (G) - \frac{2r}{s}\ M_1\ (G_1)$.

$\mathrm{IR1}\ (G_1) = \sum_{pq\in E}(d_p{}^2 + d_q{}^2) - \frac{2r}{s}\sum_{pq\in E}(d_p+d_q)$.

$\mathrm{IR1}\ (Cu_2O\ [m;\ n]) = (4m+4n-4)(1^2+2^2) + (4mn-4m-4n+4)(2^2+2^2) + 4mn(2^2+4^2) - \frac{2r}{s}(40mn-4m-4n+4)$.

$= (4m+4n-4)(1+4) + (4mn-4m-4n+4)(4+4) + 4mn(4+16) - \frac{2(8mn)}{7mn+2m+2n+2}(40mn-4m-4n+4)$.

$= 5(4m+4n-4) + 8(4mn-4m-4n+4) + 20(4mn) - \frac{16mn}{7mn+2m+2n+2}(40mn-4m-4n+4)$

$= 112mn-12m-12n+12 + \frac{-640m^2n^2+64m^2n+64mn^2-64mn}{7m+2m+2n+2}$.

$= \frac{(7mn+2m+2n+2)(112mn-12m-12n+12)-640m^2n^2+64m^2n+64mn^2-64mn}{7m+2m+2n+2}$.

$= \frac{784m^2n^2-84m^2n-84mn^2+84mn+224m^2n-24m^2-24mn+24m+224mn^2 -24mn-24n^2+24n+224mn-24m-24n+24-640m^2n^2+64m^2n+64mn^2-64mn}{7mn+2m+2n+2}$.

$\Rightarrow \mathrm{IR1}\ (Cu_2\ [m;\ n]) = \frac{144m^2n^2+204m^2n+204mn^2+196mn-24m^2-24n^2+24}{7m+2m+2n+2}$.

Theorem 13: *Let G be a graph of copper [I] oxide then its irregularity index IR2 computed as*

Proof: We know that,

$\mathrm{IR2}\ (G_1) = \sqrt{\frac{M_2(G)}{r}} - \frac{2r}{s}$ & $M_2\ (G_1) = \sum_{pq\in E}(d_p.d_q)$.

$M_2\ (Cu_2O\ [m;\ n]) = (4m+4n-4)(1\ .\ 2) + (4mn-4m-4n+4)(2\ .\ 2) + (4mn)(2\ .\ 4) = 2(4m+4n-4) + 4(4mn-4m-4n+4) + 8(4mn)$.

$= 8m+8n-8+16mn-16m-16n+16+32mn$.

$\Rightarrow M_2\ (Cu_2O\ [m;\ n]) = 48mn-8m-8n+8$.

$\mathrm{IR2}\ (Cu_2O\ [m;\ n]) = \sqrt{\frac{48mn-8m-8n+8}{8mn}} - \frac{2(8mn)}{7mn+2m+2n+2}$.

$\Rightarrow \mathrm{IR2}\ (Cu_2O\ [m;\ n]) = \sqrt{\frac{6mn-m-n+1}{mn}} - \frac{16mn}{7mn+2m+2n+2}$.

Theorem 14: *Let G be a graph of copper [I] oxide then its irregularity index IRFW computed as*

Proof: We know that,

$\mathrm{IRFW}\ (G_1) = \frac{\mathrm{IRF}\ (G)}{M_2\ (G)}$.

$\mathrm{IRFW}\ (Cu_2O\ [m;\ n]) = \frac{16mn+4m+4n-4}{48mn-8m-8n+8}$.

$\Rightarrow \mathrm{IRFW}\ (Cu_2O\ [m;\ n]) = \frac{4mn+m+n-1}{12mn-2m-2n+2}$.

Theorem 15: *Let G be a graph of copper [I] oxide then its irregularity index IRC computed as*

Proof: We know that,

$\mathrm{IRC}\ (G_1) = \sum_{pq\in E}\frac{\sqrt{d_p.d_q}}{r} - \frac{2r}{s}$.

$\mathrm{IRC}\ (Cu_2O\ [m;\ n]) = \frac{(4m+4n-4)\sqrt{1\ .\ 2} + (4mn-4m-4n+4)\sqrt{2\ .\ 2} + (6mn)\sqrt{2\ .\ 4}}{r} - \frac{2r}{s}$.

$= \frac{(4m+4n-4)\sqrt{2}+2(4mn-4m-4n+4)+6mn(2\sqrt{2})}{8mn} - \frac{2(8mn)}{7mn+2m+2n+2}$.

$= \frac{(4m+4n-4)\sqrt{2}+8mn-8m-8n+8+12mn\sqrt{2}}{8mn} - \frac{16mn}{7mn+2m+2n+2}$.

$\Rightarrow \mathrm{IRC}\ (Cu_2O\ [m;\ n]) = \frac{(12mn+4m+4n-4)\sqrt{2}+8mn-8m-8n+8}{8mn} - \frac{16mn}{7mn+2m+2n+2}$.

5. Numerical Computations of Irregularity Indices of Copper [I]

We have computed the following numerical computation from Table 2 for irregularity indices of copper [I] shown in Figure 4-8.

6. Regression Model

A regression model is a statistical method that describes the relationship between one dependent variable and one or more independent variables.

$$P = a + bX$$

$$a = \frac{(\sum y)(\sum x^2) - (\sum x)(\sum xy)}{n(\sum x^2) - (\sum x)^2}$$

$$b = \frac{n(\sum xy) - (\sum x)(\sum y)}{n(\sum x^2) - (\sum x)^2}$$

Where P is the dependent variable and X is the independent variable. The variable P represents the physical or chemical properties and X represents the irregularity indices. The term "a" is the intercept and the "b" is slope. We computed physicochemical properties of copper [I] Oxide by using irregularity indices. Boiling point of copper [I] oxide is 1800°C. Enthalpy of copper [I] oxide is –168.6 kJ/mol. Molar

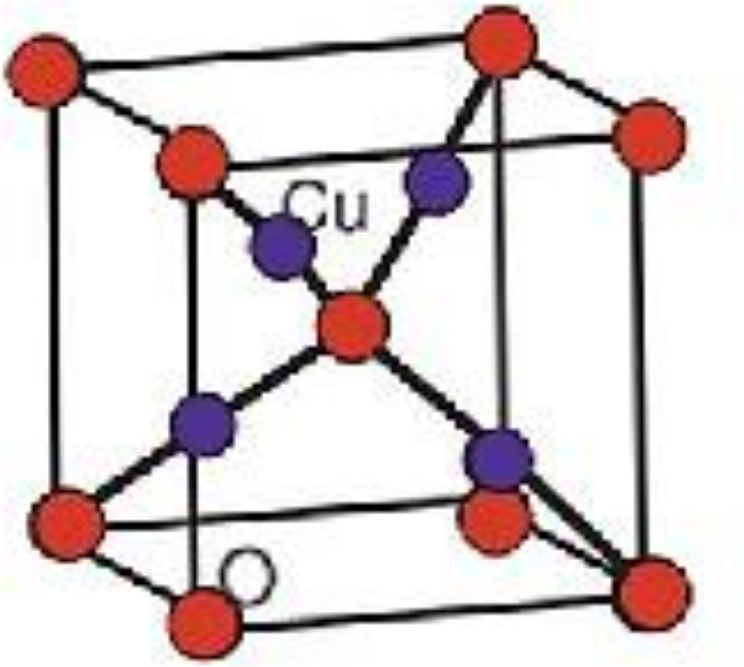

Figure 1. Cu_2O [1; 1]

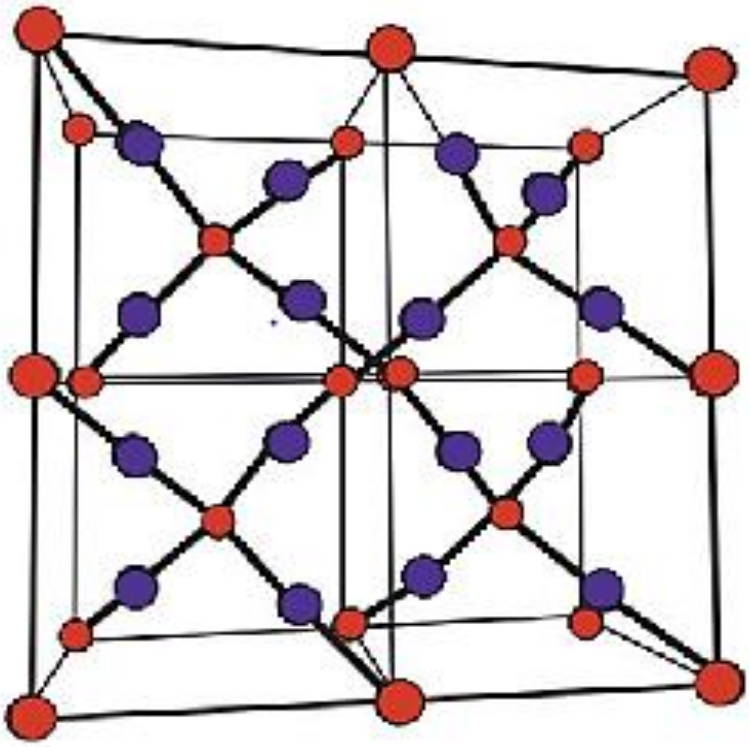

Figure 2. Cu_2O [2; 2]

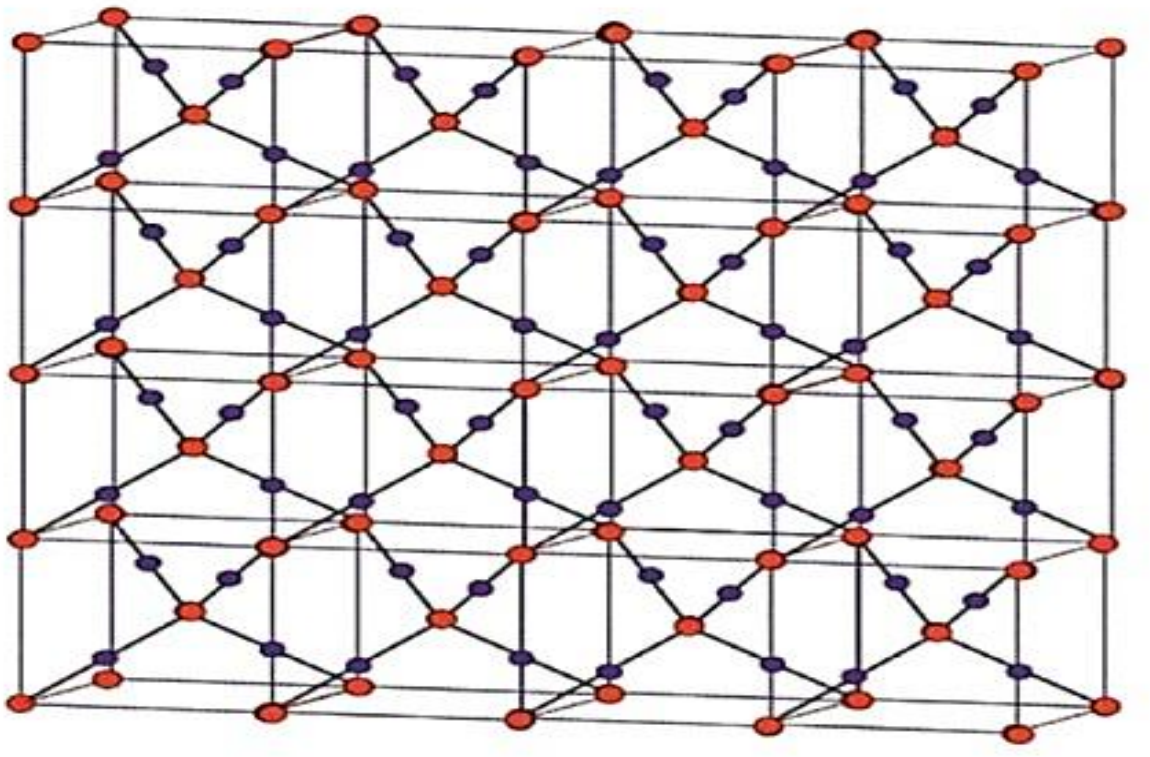

Figure 3. Cu_2O [4; 4]

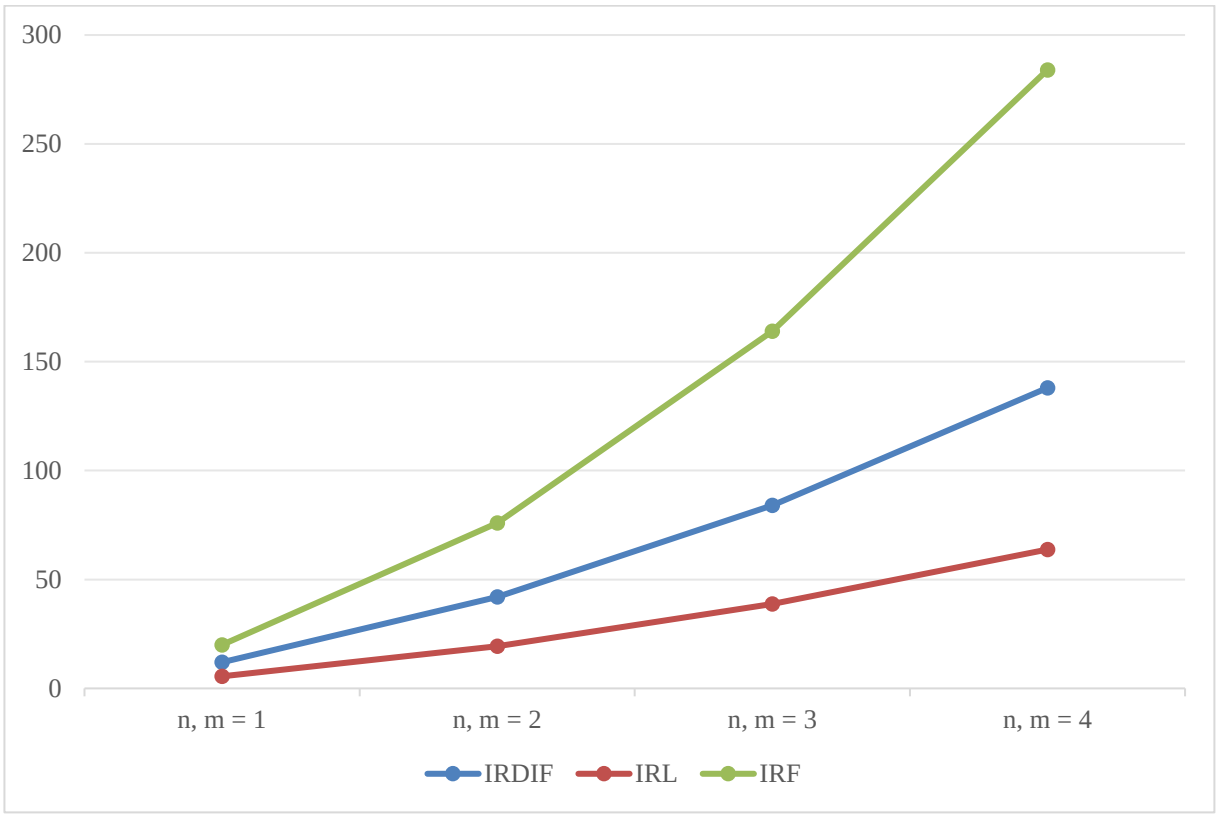

Figure 4. IRDIF, IRL and IRF of Cu_2O [m; n]

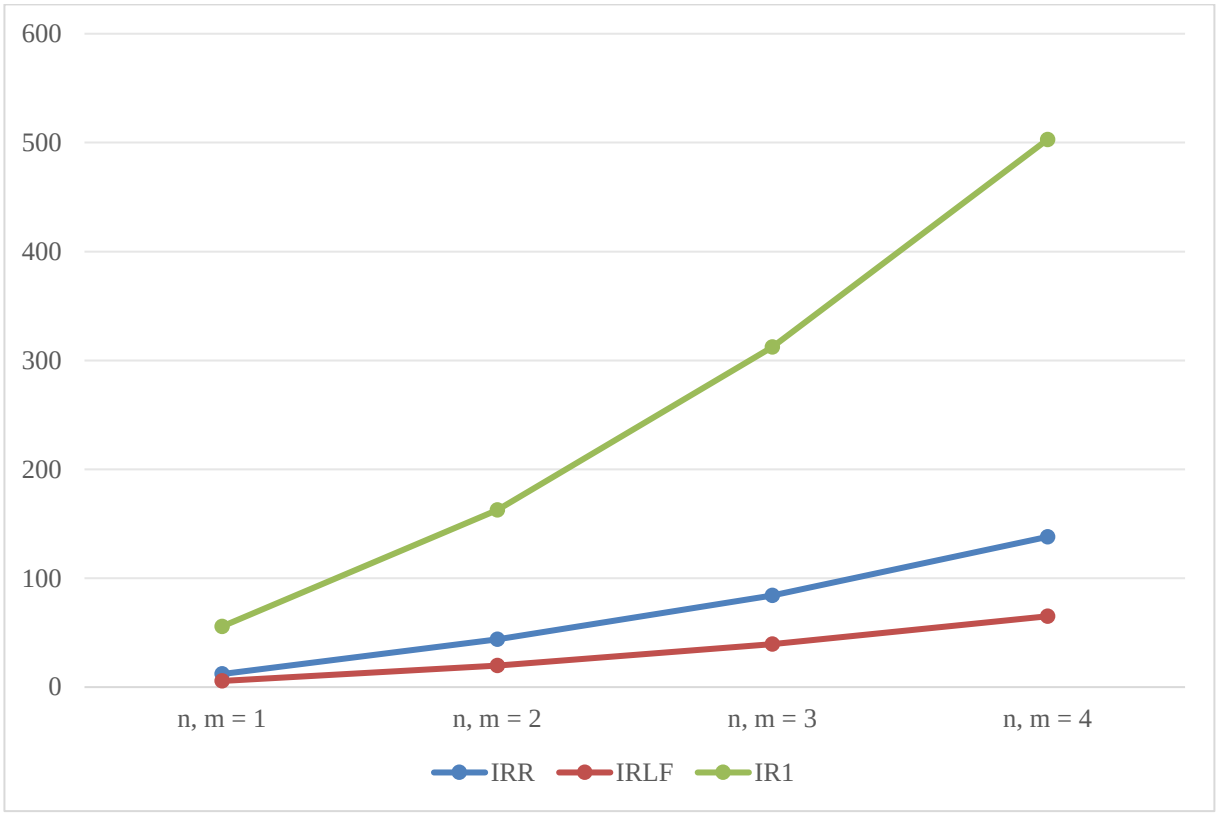

Figure 5. IRR, IRLF and IR1 of Cu_2O [m; n]

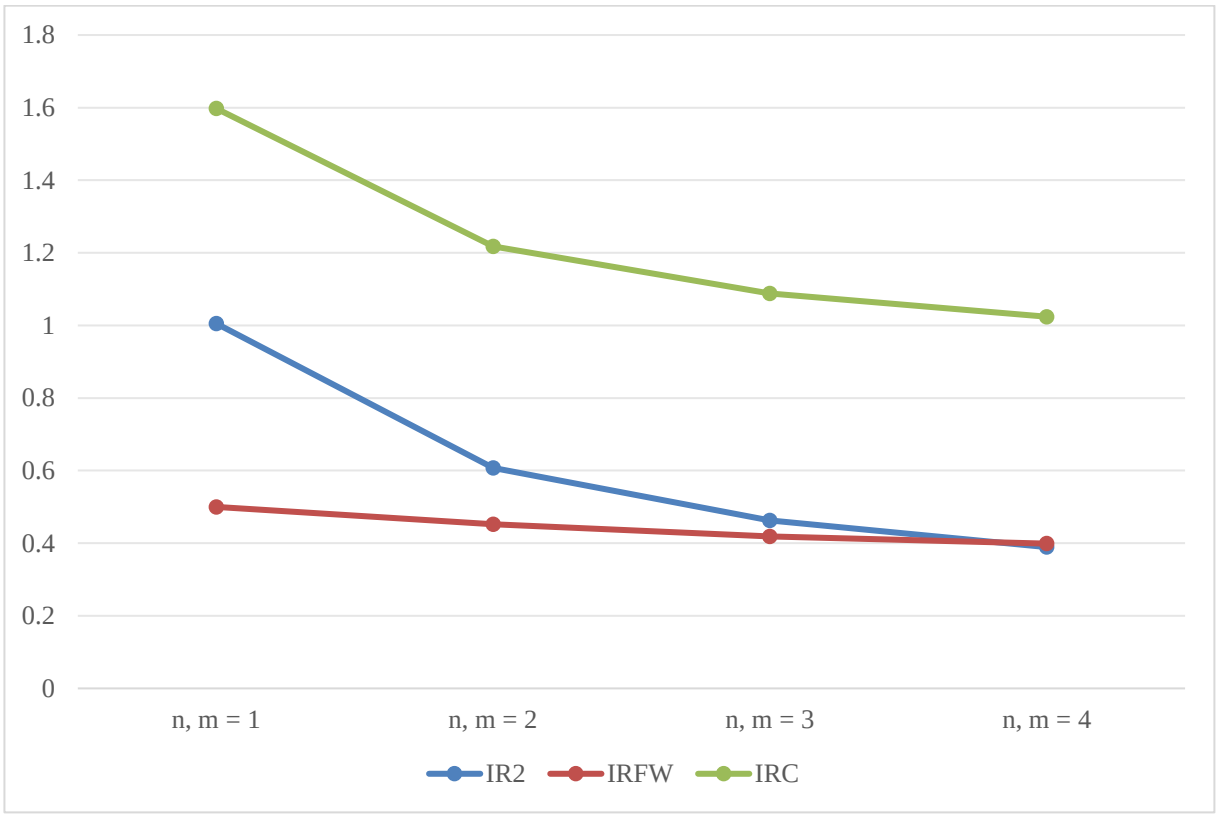

Figure 6. IR2, IRFW and IRC of Cu_2O [m; n]

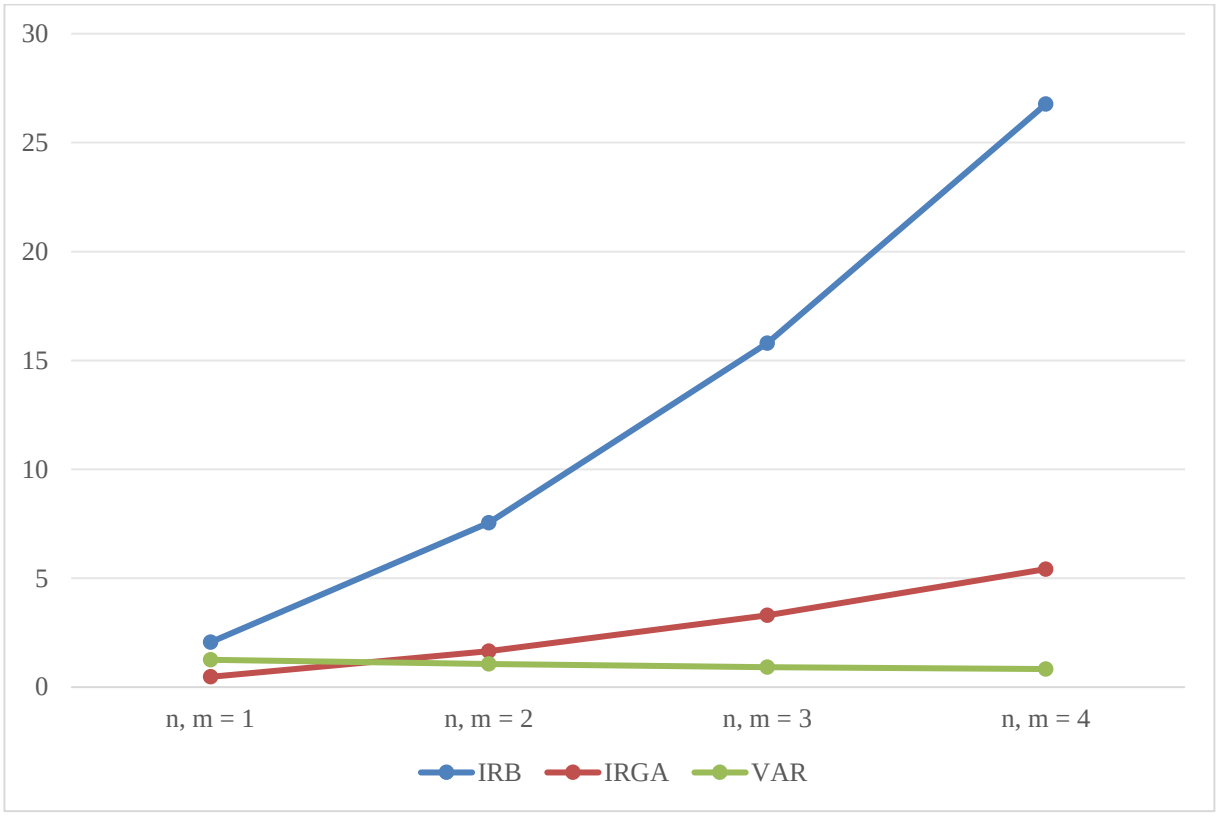

Figure 7. IRB, IRGA and VAR of Cu_2O [m; n]

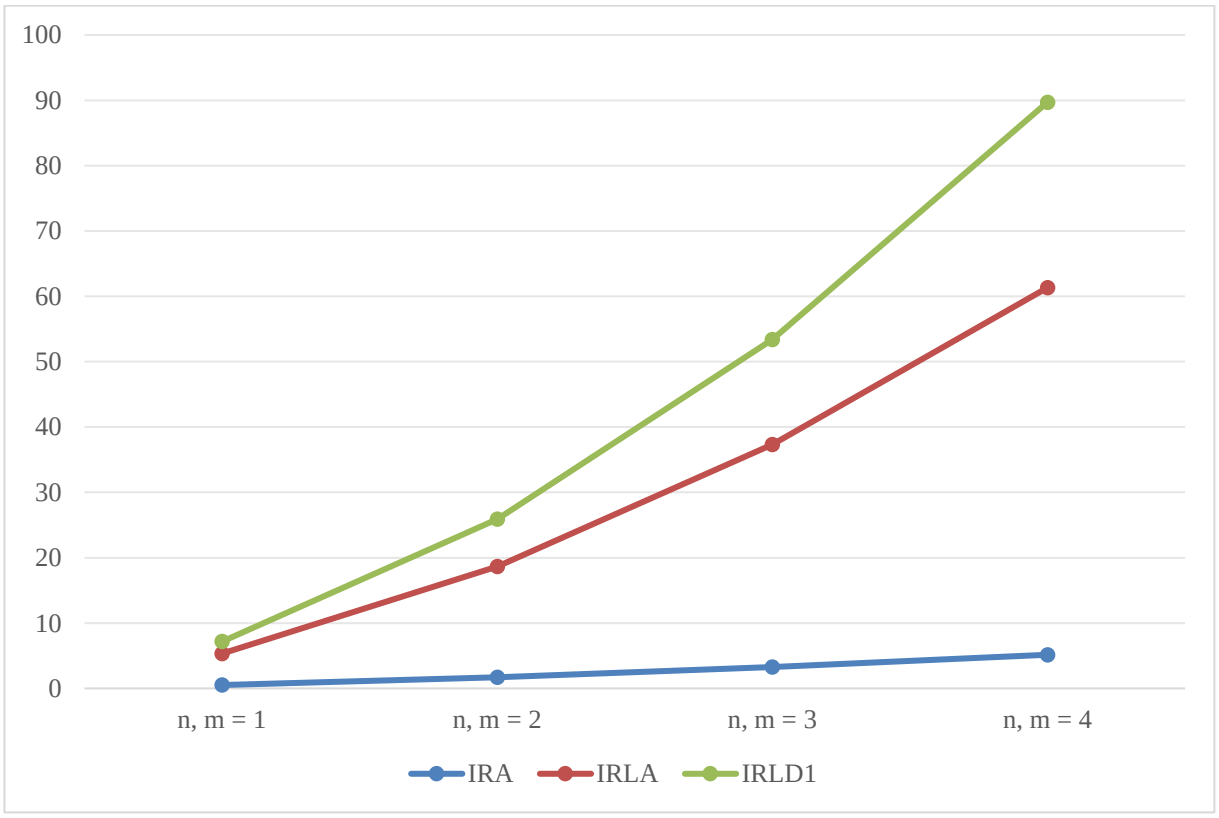

Figure 8. IRA, IRLA and IRLD_1 of Cu_2O [m; n]

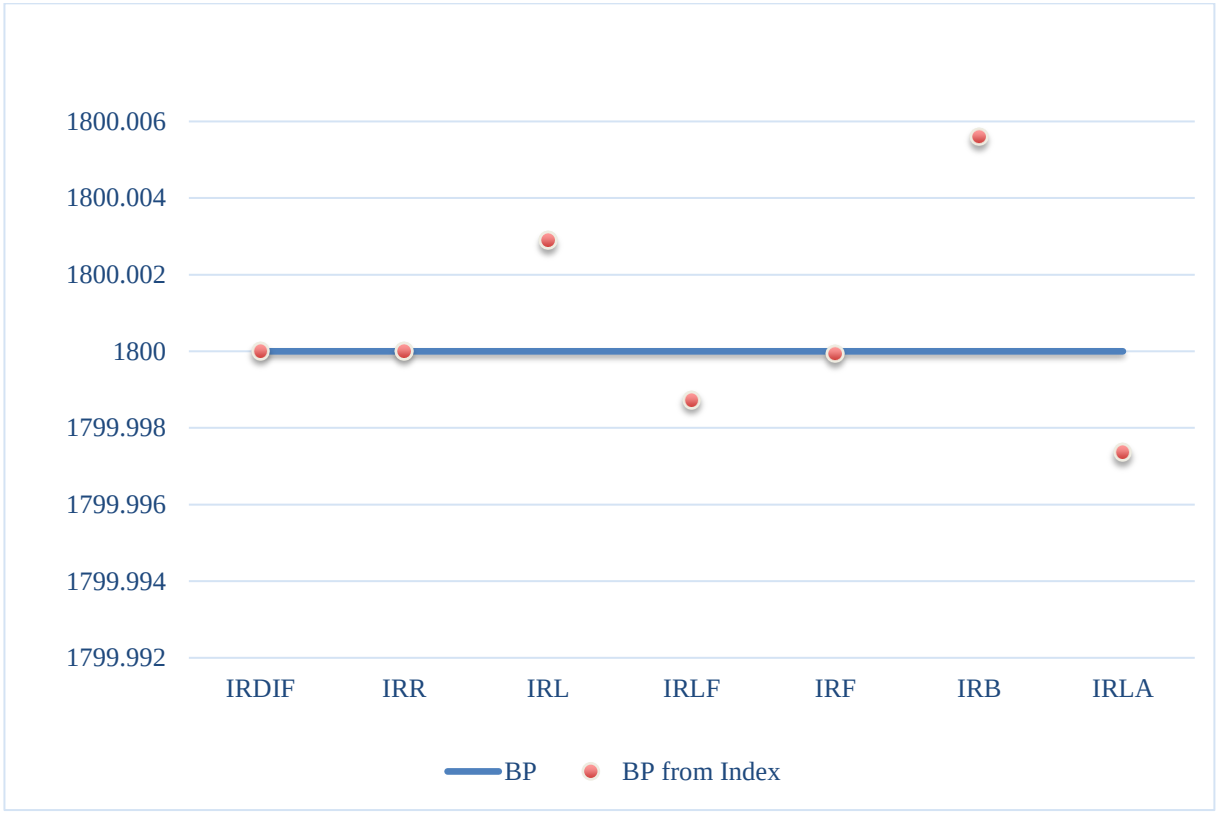

Figure 9. Comparison of boiling point of Cu_2O [m; n] with boiling point computed from IRDIF, IRR, IRL, IRLF, IRF, IRB and IRLA.

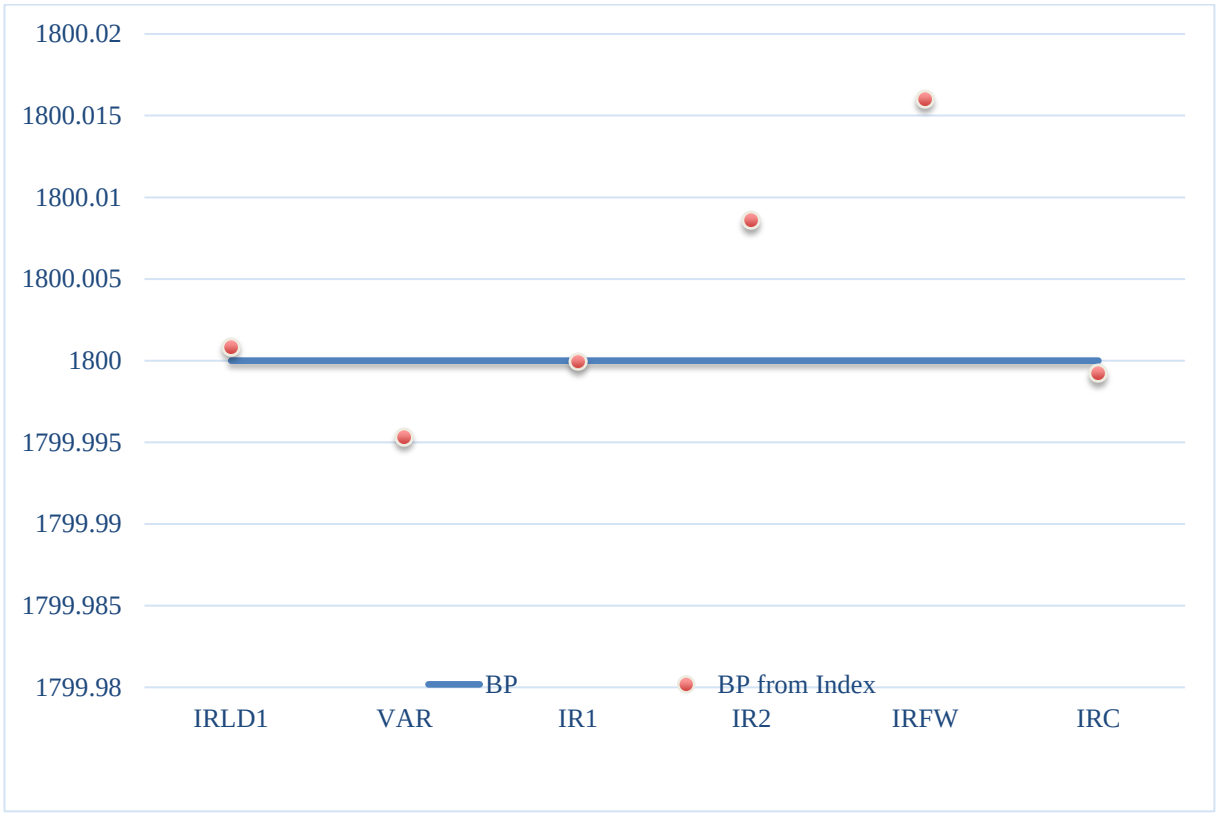

Figure 10. Comparison of boiling point of Cu_2O [m; n] with boiling point computed from $IRLD_1$, VAR, IR1, IR2, IRFW and IRC.

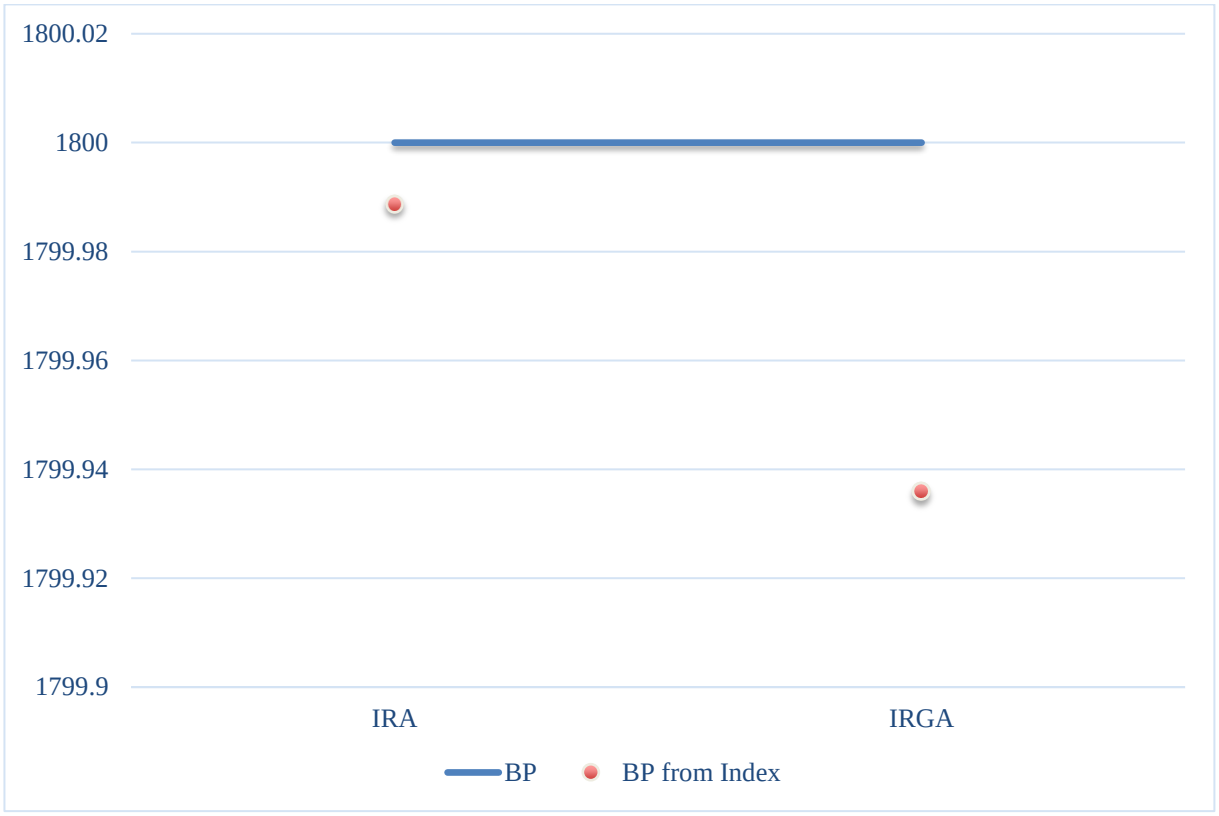

Figure 11. Comparison of boiling point of Cu_2O [m; n] with boiling point computed from IRA and IRGA.

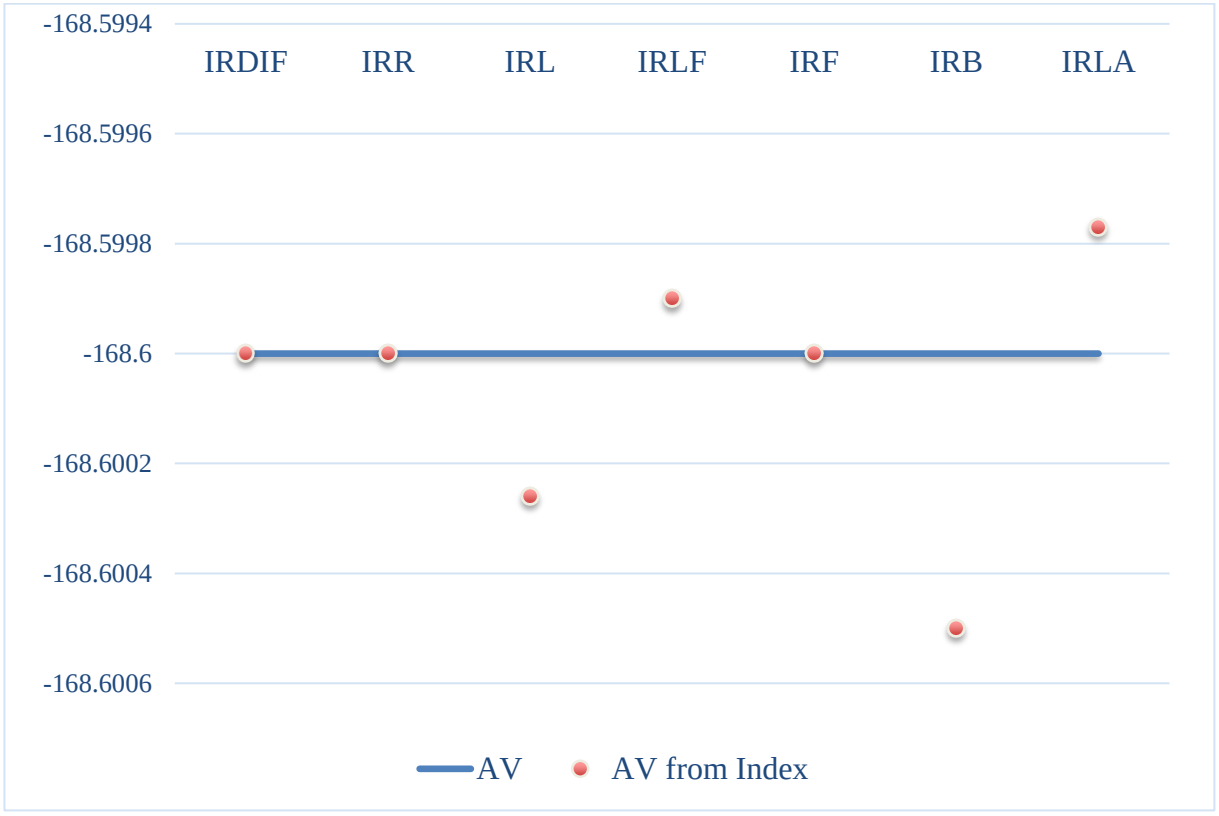

Figure 12. Comparison of enthalpy of Cu_2O [m; n] with enthalpy computed from IRDIF, IRR, IRL, IRLF, IRF, IRB and IRLA.

Figure 13. Comparison of enthalpy of Cu_2O [m; n] with enthalpy computed from $IRLD_1$, VAR, IR1, IR2, IRFW and IRC.

Figure 14. Comparison of enthalpy Cu_2O [m; n] of with enthalpy computed from IRA and IRGA.

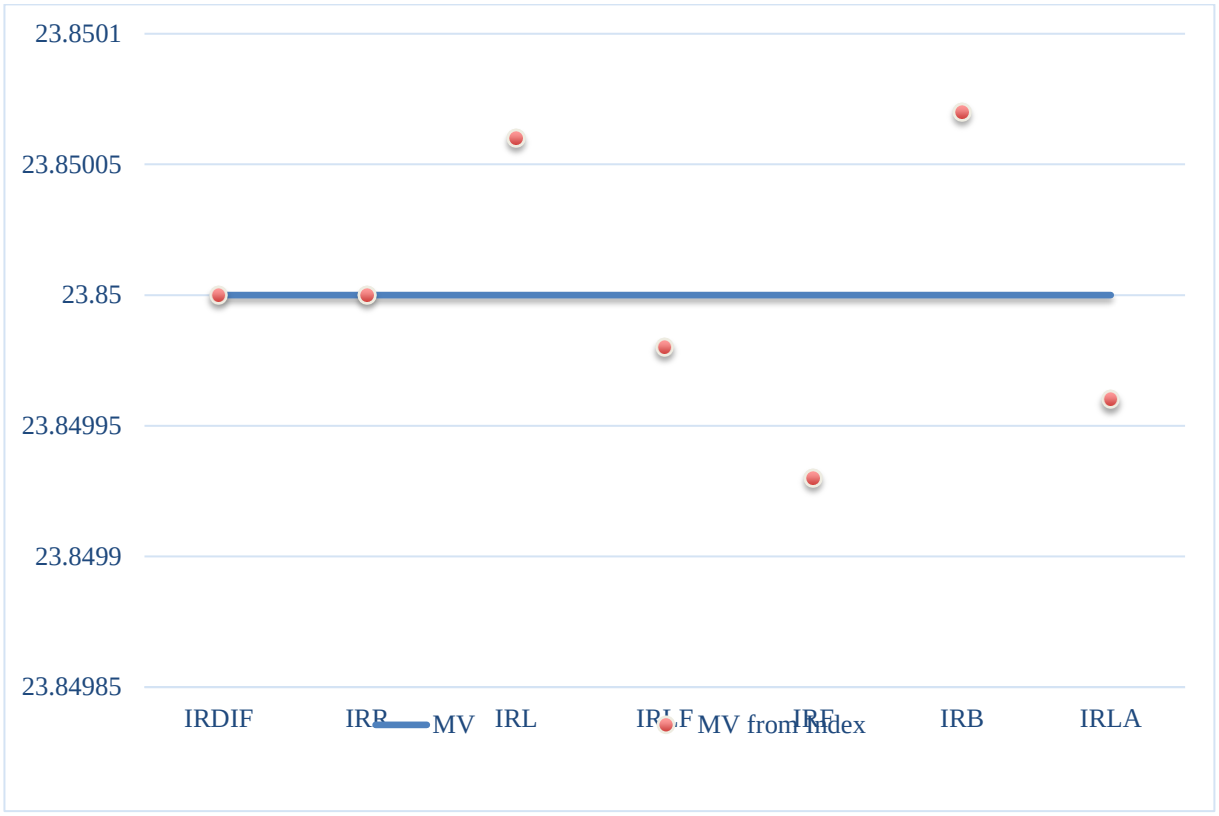

Figure 15. Comparison of molar volume of Cu_2O [m; n] with molar volume computed from IRDIF, IRR, IRL, IRLF, IRF, IRB and IRLA.

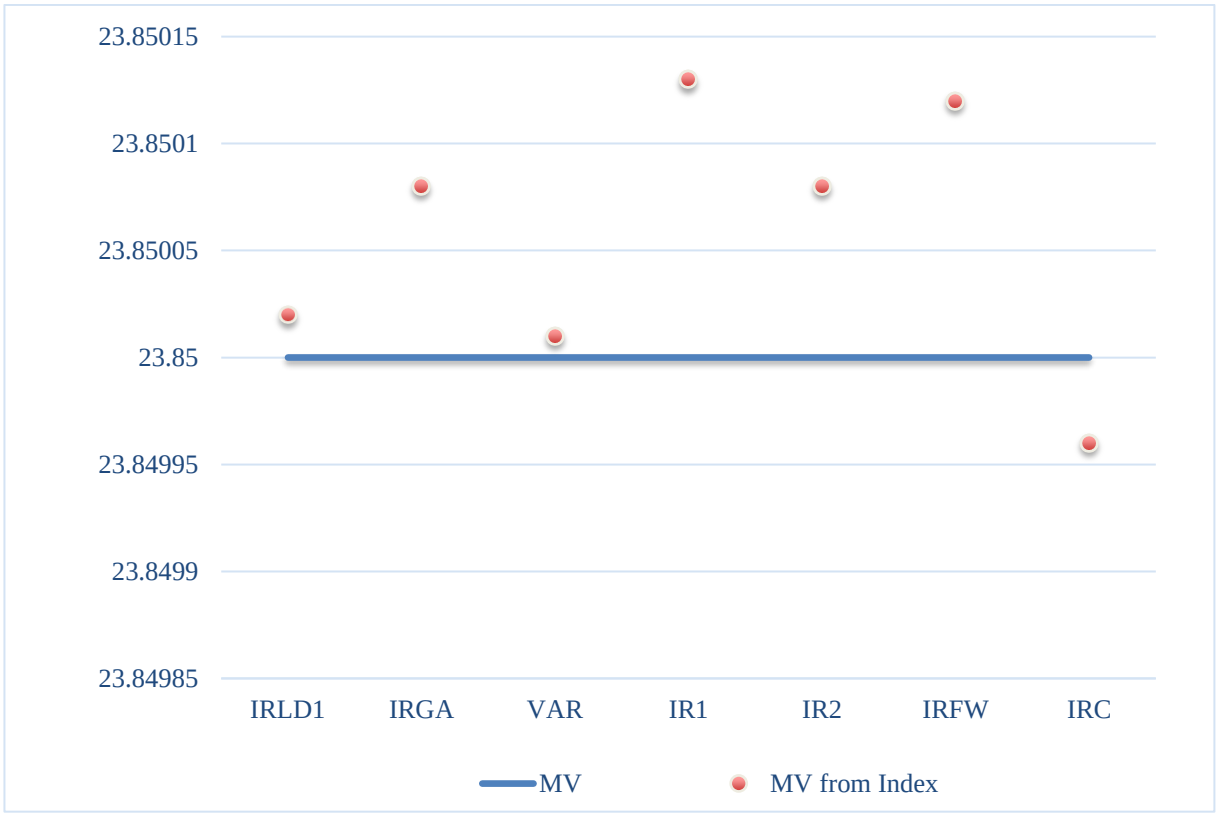

Figure 16. Comparison of molar volume of Cu_2O [m; n] with molar volume computed from $IRLD_1$, IRGA, VAR, IR1, IR2, IRFW and IRC.

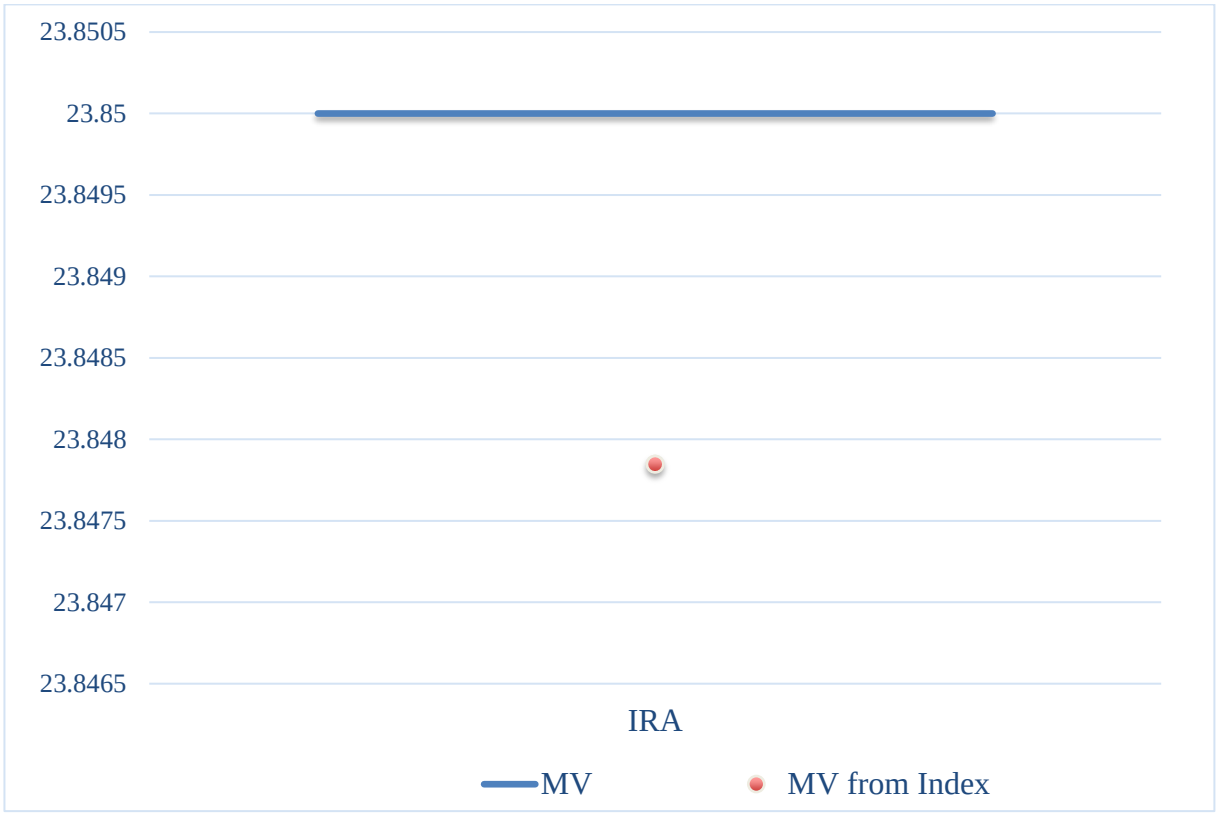

Figure 17. Comparison of molar volume of Cu_2O [m; n] with molar volume computed from IRA.

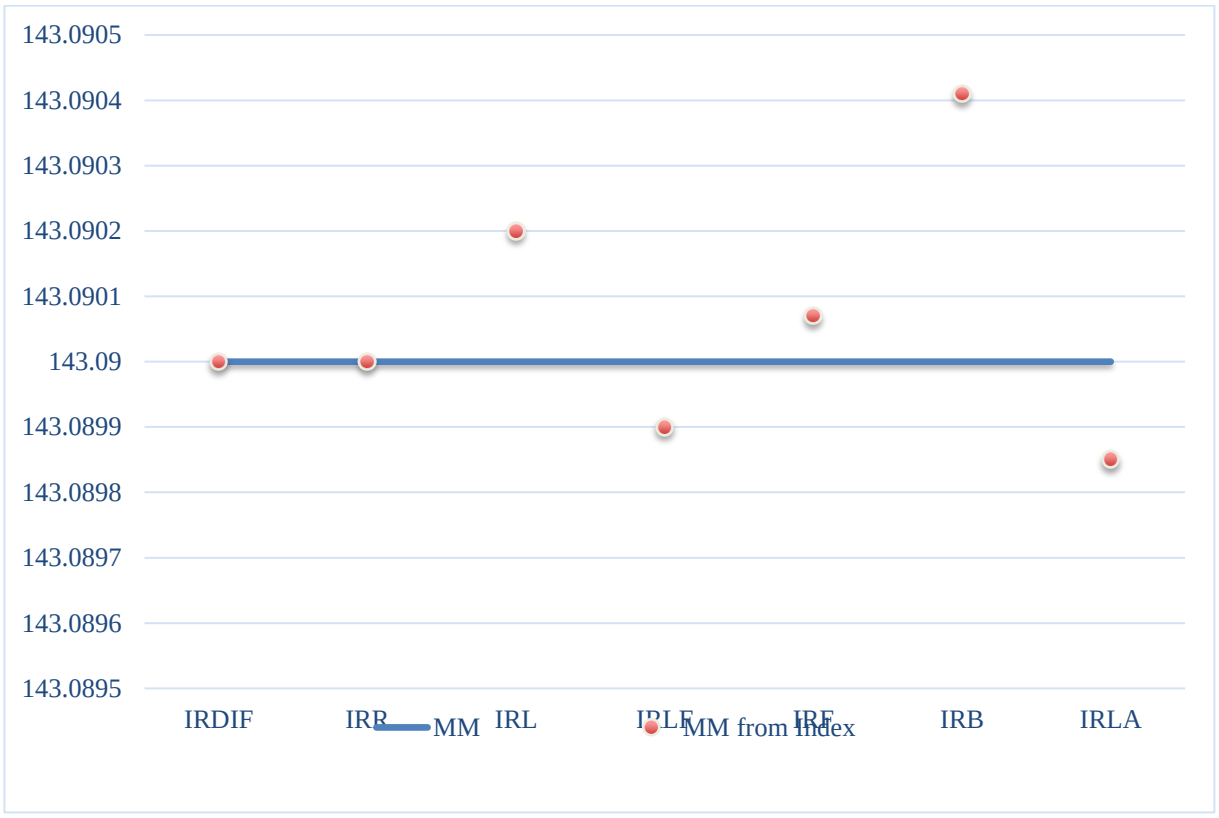

Figure 18. Comparison of molar mass of Cu_2O [m; n] with molar mass computed from IRDIF, IRR, IRL, IRLF, IRF, IRB and IRLA.

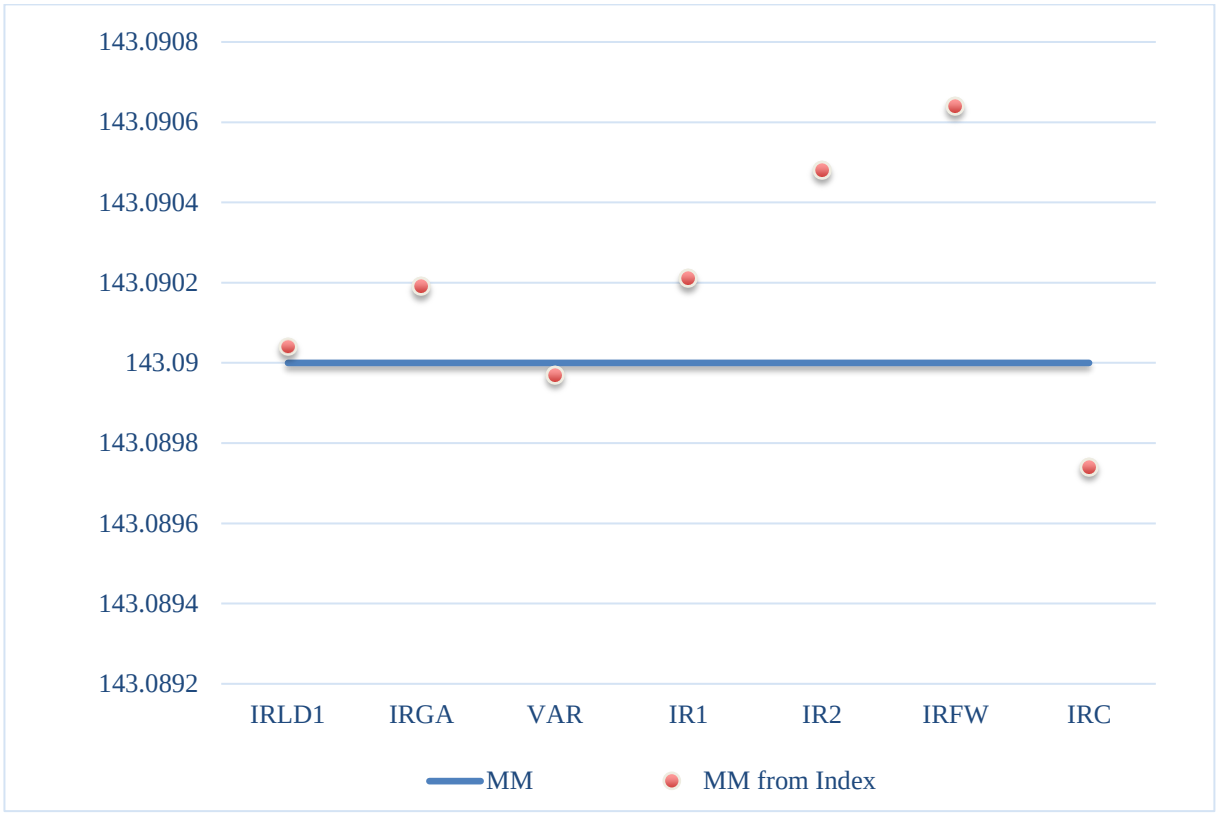

Figure 19. Comparison of molar mass of Cu_2O [m; n] with molar mass computed from $IRLD_1$, IRGA, VAR, IR1, IR2, IRFW and IRC.

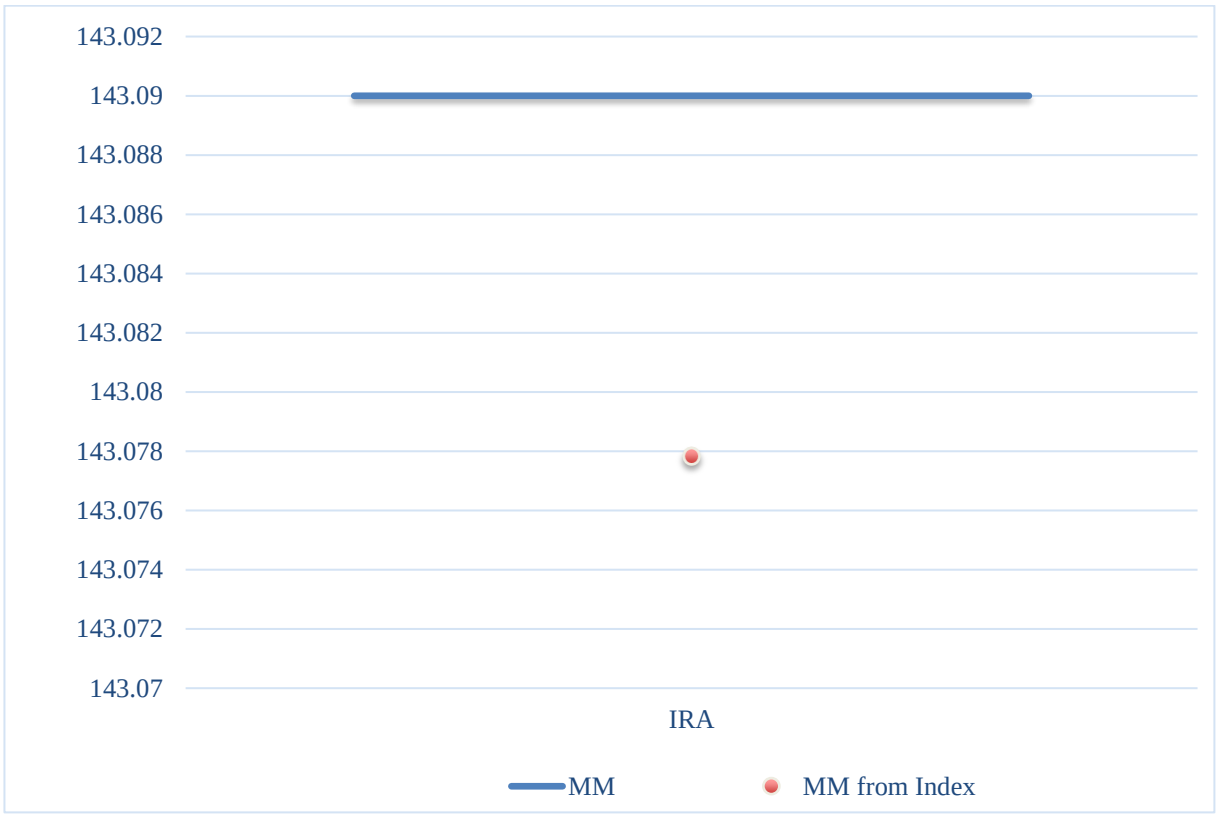

Figure 20. Comparison of molar mass of Cu_2O [m; n] with molar mass computed from IRA.

Table 1. Edge partition of $G_1 \approx Cu_2O$ [m; n]

Number of edges (d_p, d_q)	Number of indices
(1, 2)	4m + 4n – 4
(2, 2)	4mn – 4m – 4n + 4
(2, 4)	4mn

Table 2. Numerical computation of irregularity indices of copper [I] oxide for n = 1, 2, 3, 4 & m = 1, 2, 3, 4

Irregularity Indices	n, m = 1	n, m = 2	n, m = 3	n, m = 4
IRDIF (G_1)	12	42	84	138
IRR (G_1)	12	44	92	156
IRL (G_1)	5.54517	19.40812	38.81624	63.76954
IRLF (G_1)	5.65685	19.79898	39.59797	65.05382
IRF (G_1)	20	76	164	284
IRA (G_1)	0.51471	1.71572	3.25988	5.14718
IRB (G_1)	2.05887	7.54920	15.78470	26.76537.
IRLA (G_1)	5.33333	18.66667	37.33333	61.33333
$IRLD_1$ (G_1)	7.16703	25.89556	53.41298	89.71930
IRGA (G_1)	0.47113	1.64896	3.29792	5.41801
VAR (G_1)	1.25443	1.05817	0.91752	0.82982
IR1 (G_1)	55.69231	162.73684	312.15584	502.83077
IR2 (G_1)	1.00530	0.60708	0.46320	0.38926
IRFW (G_1)	0.5	0.45238	0.41837	0.39888
IRC (G_1)	1.59766	1.21744	1.08847	1.02395

Table 3. Physicochemical properties of copper [I] oxide

npound				I
Cu_2O	0	8.6	5	09

Table 4. Computation of boiling point of copper [I] oxide from each irregularity indices

Irregularity Indices	Cu_2O	a	b
IRDIF	12	2400	–50
IRR	12	2400	–50
IRL	5.54517	2442.51935	–115.86957
IRLF	5.65685	2430.93810	–111.53546
IRF	20	2133.33333	–16.66667
IRA	0.51471	2225.02825	–825.78445
IRB	2.05887	2171.10755	–180.24545
IRLA	5.33333	2466.66361	–125
$IRLD_1$	7.16703	2683.80458	–123.31520
IRGA	0.47113	2208.09537	–866.34146
VAR	1.25443	2072.37349	–217.13302
IR1	55.69231	2040.26547	–4.31416
IR2	1.00530	2037.93516	–236.67222
IRFW	0.5	2080.016	–560
IRC	1.59766	2017.28536	–136.00274

Table 5. Computation of enthalpy of copper [I] oxide from each irregularity indices

Irregularity Indices	Cu_2O	a	b
IRDIF	12	–132.6	–3
IRR	12	–132.6	–3
IRL	5.54517	–130.04929	–6.95217
IRLF	5.65685	–130.74352	–6.69213
IRF	20	–148.6	–1
IRA	0.51471	–143.09222	–49.54707
IRB	2.05887	–146.33440	–10.81472
IRLA	5.33333	–128.59979	–7.5
$IRLD_1$	7.16703	–115.57185	–7.39891
IRGA	0.47113	–144.10644	–51.98056
VAR	1.25443	–152.25697	–13.02801
IR1	55.69231	–154.18407	–0.25885
IR2	1.00530	–154.32513	–14.20033
IRFW	0.5	–151.80123	–33.60006
IRC	1.59766	–155.56267	–8.16017

Table 6. Computation of molar volume of copper [I] oxide from each irregularity indices

Irregularity Indices	Cu_2O	a	b
IRDIF	12	–9.912	2.8135
IRR	12	–9.912	2.8135
IRL	5.54517	–12.30439	6.51999
IRLF	5.65685	–11.65298	6.27610
IRF	20	5.09333	0.93783
IRA	0.51471	–0.069	46.46665
IRB	2.05887	2.96815	10.14242
IRLA	5.33333	–13.66335	7.03375
$IRLD_1$	7.16703	–25.88164	6.93895
IRGA	0.47113	0.88294	48.74905
VAR	1.25443	8.52326	12.21810
IR1	55.69231	10.33026	0.24276
IR2	1.00530	10.46194	13.31756
IRFW	0.5	8.09447	31.51129
IRC	1.59766	11.62326	7.65288

Table 7. Computation of molar mass of copper [I] oxide from each irregularity indices

Irregularity Indices	Cu_2O	a	b
IRDIF	12	–47.545	15.88625
IRR	12	–47.545	15.88625
IRL	5.54517	–61.05335	36.81466
IRLF	5.65685	–57.37534	35.43761
IRF	20	37.18167	5.29542
IRA	0.51471	8.03224	262.37218
IRB	2.05887	25.18203	57.26849
IRLA	5.33333	–68.72671	39.71563
$IRLD_1$	7.16703	–137.7164	39.18032
IRGA	0.47113	13.40769	275.25842
VAR	1.25443	56.54859	68.98861
IR1	55.69231	66.75165	1.37072
IR2	1.00530	67.49524	75.19670
IRFW	0.5	54.12763	177.92602
IRC	1.59766	74.05249	43.21148

Table 8. Computation of molar mass of copper [I] oxide from each irregularity indices

	BP	**EV**	**MV**	**MM**
IRDIF (G_1)	2400 – 50[IRDIF(G_1)]	–132.6 – 3[IRDIF(G_1)]	–9.9 + 2.8[IRDIF(G_1)]	– 47.5 + 15.8[IRDIF(G_1)]
IRR (G_1)	2400 – 50[IRR(G_1)]	–132.6 – 3[IRR(G_1)]	–9.9 + 2.8[IRR(G_1)]	– 47.5 + 15.8[IRR(G_1)]
IRL (G_1)	2442.51 – 115.8[IRL(G_1)]	–130.0 – 6.9[IRL(G_1)]	–12.3 + 6.5[IRL(G_1)]	–61.0+36.8[IRL(G_1)]
IRLF (G_1)	2430.9 – 111.5[IRLF(G_1)]	–130.7 – 6.6[IRLF(G_1)]	–11.6 + 6.2[IRLF(G_1)]	–57.3 + 35.4[IRLF(G_1)]
IRF (G_1)	2133.3 – 16.6[IRF(G_1)]	–148.6 – 1[IRF(G_1)]	5.1 + 0.9[IRF(G_1)]	37.1 + 5.3[IRF(G_1)]
IRA (G_1)	2225.0 – 825.7[IRA(G_1)]	–143.1 – 49.5[IRA(G_1)]	–0.06 + 46.4[IRA(G_1)]	8.0 + 262.3[IRA(G_1)]
IRB (G_1)	2171.1 – 180.2[IRB(G_1)]	–146.3 – 10.8[IRB(G_1)]	2.9 + 10.1[IRB(G_1)]	25.1 +57.2[IRB(G_1)]
IRLA (G_1)	2466.6 – 125[IRLA(G_1)]	–128.6 – 7.5[IRLA(G_1)]	–13.6 + 7.0[IRLA(G_1)]	–68.7 + 39.7[IRLA(G_1)]
$IRLD_1$ (G_1)	2683.8 – 123.3[$IRLD_1$(G_1)]	–115.5 – 7.3[$IRLD_1$(G_1)]	–25.8 + 6.9[$IRLD_1$(G_1)]	–137.7 + 39.1[$IRLD_1$(G_1)]
IRGA (G_1)	2208.1 – 866.3[IRGA(G_1)]	–144.1 – 51.9[IRGA(G_1)]	0.8 + 48.7[IRGA(G_1)]	13.4 + 275.2[IRGA(G_1)]
VAR (G_1)	2072.3 – 217.1[VAR(G_1)]	–152.2 – 13.0[VAR(G_1)]	8.5 + 12.2[VAR(G_1)]	56.5 + 68.9[VAR(G_1)]
IR1 (G_1)	2040.2 – 4.3[IR1(G_1)]	–154.1 – 0.2[IR1(G_1)]	10.3 + 0.2[IR1(G_1)]	66.7 + 1.3[IR1(G_1)]
IR2 (G_1)	2037.9 – 236.6[IR2(G_1)]	–154.3 – 14.2[IR2(G_1)]	10.4 + 13.3[IR2(G_1)]	67.4 + 75.1[IR2(G_1)]
IRFW (G_1)	2080.0 – 560[IRFW(G_1)]	–151.8 – 33.6[IRFW(G_1)]	8.1 + 31.5[IRFW(G_1)]	54.1 + 177.9[IRFW(G_1)]
IRC (G_1)	2017.2 – 136.0[IRC(G_1)]	–155.5 – 8.1[IRC(G_1)]	11.6 + 7.6[IRC(G_1)]	74.0 + 43.2[IRC(G_1)]

Volume of copper [I] oxide is 23.85 cm^3/mol. Molar mass of copper [I] oxide is 143.09 g/mol.

7. Computation of physicochemical properties of copper [I] oxide by using each irregularity indices

In Table 8, we have computed BP, EV, MV and MM using all irregularity indices. Comparison of physiochemical properties depicted in Figures 9-20.

8. Conclusions

In this study, we have computed irregularity indices for copper [I] oxide Cu_2O [m; n] for n = 1, 2, 3, 4 and m = 1, 2, 3, 4. We have generated the n^{th} term formula. We have also computed physicochemical properties like boiling point, enthalpy, molar volume and molar mass of and from calculated values of irregularity indices by using regression models. We have drawn the comparison of experimental values of boiling point, enthalpy, molar volume and molar mass of copper [I] oxide with the theoretical values of the boiling point, enthalpy, molar volume and molar mass calculated with the help of irregularity indices.

References

[1] P. Zhang, G. Chartrand. (2006). Introduction to graph theory. Tata McGraw-Hill. 2: 2.1.

[2] R. García-Domenech, J. Gálvez, J.V. de Julián-Ortiz, L. Pogliani. (2008). Some new trends in chemical graph theory. Chemical Reviews. 108(3): 1127-1169.

[3] J. Singh, G. Kaur, M. Rawat. (2016). A brief review on synthesis and characterization of copper oxide nanoparticles and its applications. J. Bioelectron. Nanotechnol. 1(9).

[4] K. Akimoto, S. Ishizuka, M. Yanagita, Y. Nawa, G.K. Paul, T. Sakurai. (2006). Thin film deposition of Cu2O and application for solar cells. Solar energy. 80(6): 715-722.

[5] C.-Y. Huang, X.-R. He. (2022). Easily processable Cu2O/Si self-powered photodetector array for image sensing applications. ACS Applied Electronic Materials. 4(3): 1335-1342.

[6] D. Gupta, S. Meher, N. Illyaskutty, Z.C. Alex. (2018). Facile synthesis of Cu2O and CuO nanoparticles and study of their structural, optical and electronic properties. Journal of Alloys and Compounds. 743: 737-745.

[7] H. Al-Jawhari. (2015). A review of recent advances in transparent p-type Cu2O-based thin film transistors. Materials Science in Semiconductor Processing. 40: 241-252.

[8] Q. Su, C. Zuo, M. Liu, X. Tai. (2023). A review on Cu2O-based composites in photocatalysis: synthesis, modification, and applications. Molecules. 28(14): 5576.

[9] P.P. Janantha, L. Perera, K. Jayathilaka, J. Jayanetti, D. Dissanayaka, W. Siripala In *Use of Cu2O microcrystalline thin film semiconductors for gas sensing*, Proceedings of the Technical Sessions, 2009; 2009; pp 70-76.

[10] C. Li, M. Atlar, M. Haroutunian, R. Norman, C. Anderson. (2019). An investigation into the effects of marine biofilm on the roughness and drag characteristics of surfaces coated with different sized cuprous oxide (Cu2O) particles. Biofouling. 35(1): 15-33.

[11] S. Bijani, M. Gabás, L. Martínez, J. Ramos-Barrado, J. Morales, L. Sánchez. (2007). Nanostructured Cu2O thin film electrodes prepared by electrodeposition for rechargeable lithium batteries. Thin Solid Films. 515(13): 5505-5511.

[12] M.A. Bhosale, B.M. Bhanage. (2016). A simple approach for sonochemical synthesis of Cu2O

nanoparticles with high catalytic properties. Advanced Powder Technology. 27(1): 238-244.

[13] J. An, Q. Zhou. (2012). Degradation of some typical pharmaceuticals and personal care products with copper-plating iron doped Cu2O under visible light irradiation. Journal of Environmental Sciences. 24(5): 827-833.

[14] M. Mallik, S. Monia, M. Gupta, A. Ghosh, M.P. Toppo, H. Roy. (2020). Synthesis and characterization of Cu2O nanoparticles. Journal of Alloys and Compounds. 829: 154623.

[15] I. Peng, K. Hills-Kimball, I.M. Lovelace, J. Wang, M. Rios, O. Chen, L.-Q. Wang. (2022). Exploring the Colors of Copper-Containing Pigments, Copper (II) Oxide and Malachite, and Their Origins in Ceramic Glazes. Colorants. 1(4): 376-387.

[16] P. Wang, X. Zhao, B. Li. (2011). ZnO-coated CuO nanowire arrays: fabrications, optoelectronic properties, and photovoltaic applications. Optics express. 19(12): 11271-11279.

[17] J. Gu, L. Li, D. Huang, L. Jiang, L. Liu, F. Li, A. Pang, X. Guo, B. Tao. (2019). In situ synthesis of graphene@ cuprous oxide nanocomposite incorporated marine antifouling coating with elevated antifouling performance. Open Journal of Organic Polymer Materials. 9(3): 47-62.

[18] N.N. Sheno, A. Morsali, S.W. Joo. (2014). Synthesis CuO nanoparticles from a copper (II) metal-organic framework precursor. Materials Letters. 117: 31-33.

[19] X. Guo, D. Mao, S. Wang, G. Wu, G. Lu. (2009). Combustion synthesis of CuO–ZnO–ZrO2 catalysts for the hydrogenation of carbon dioxide to methanol. Catalysis Communications. 10(13): 1661-1664.

[20] T. Wen, X.L. Wu, S. Zhang, X. Wang, A.W. Xu. (2015). Core–Shell Carbon-Coated CuO Nanocomposites: A Highly Stable Electrode Material for Supercapacitors and Lithium-Ion Batteries. Chemistry–An Asian Journal. 10(3): 595-601.

[21] S. Hayat, M. Imran. (2014). Computation of topological indices of certain networks. Applied Mathematics and Computation. 240: 213-228.

[22] A. Tropsha. (2010). Best practices for QSAR model development, validation, and exploitation. Molecular informatics. 29(6-7): 476-488.

[23] A.R. Katritzky, E.V. Gordeeva. (1993). Traditional topological indexes vs electronic, geometrical, and combined molecular descriptors in QSAR/QSPR research. Journal of chemical information and computer sciences. 33(6): 835-857.

[24] Z. Hussain, Y. Yang, M. Munir, Z. Hussain, M. Athar, A. Ahmed, H. Ahmad. (2020). Analysis of irregularity measures of zigzag, rhombic, and honeycomb benzenoid systems. Open Physics. 18(1): 1146-1153.

[25] I. Gutman, K.C. Das. (2004). The first Zagreb index 30 years after. MATCH Commun. Math. Comput. Chem. 50(1): 83-92.

[26] K.C. Das, I. Gutman. (2004). Some properties of the second Zagreb index. MATCH Commun. Math. Comput. Chem. 52(1): 3-1.

[27] Z. Che, Z. Chen. (2016). Lower and upper bounds of the forgotten topological index. MATCH Commun. Math. Comput. Chem. 76(3): 635-648.

[28] A. Jahanbani. (2019). Albertson energy and Albertson Estrada index of graphs. Journal of Linear and Topological Algebra. 8(01): 11-24.

[29] A. Hamzeh, T. Réti. (2014). An analogue of Zagreb index inequality obtained from graph irregularity measures. MATCH Commun. Math. Comput. Chem. 72(3): 669-683.

[30] M. Ascioglu, I.N. Cangul In *Sigma index and forgotten index of the subdivision and r-subdivision graphs*, Proceedings of the Jangjeon Mathematical Society, 2018; 2018; pp 1-14.

[31] L. Euler. (1953). Leonhard Euler and the Königsberg bridges. Scientific American. 189(1): 66-72.

[32] N.P. Johnson. (2004). The brachistochrone problem. The College Mathematics Journal. 35(3): 192-197.

[33] B.-A. Morel. (1857). Traite des degenerescences physiques, intellectuelles et morales de l'espece humaine et des causes qui produisent ces varietes maladives par le Docteur BA Morel. chez J.-B. Bailliere: pp.

[34] E.C. Kirby, R.B. Mallion, P. Pollak, P.J. Skrzyński. (2016). What Kirchhoff actually did concerning spanning trees in electrical networks and its relationship to modern graph-theoretical work. Croatica Chemica Acta. 89(4): 403-417.

[35] M.H. Aftab, I. Siddique, J.K.K. Asamoah, H.A. El-Wahed Khalifa, M. Hussain. (2022). Multiplicative attributes derived from graph invariants for saztec4 diamond. Journal of Mathematics. 2022(1): 9148581.

[36] K. Jebreen, H. Iqbal, M.H. Aftab, I. Yaqoob, M.I. Sowaity, A. Barham. (2023). Study of eccentricity based topological indices for benzenoid structure. South African Journal of Chemical Engineering. 45: 221-227.

[37] M.H. Aftab. (2023). Measuring irregularities in the chemical compound: porous graphene. Polycyclic Aromatic Compounds. 1-10.

[38] I. Ali, M.H. Aftab, M.W. Raheed, K. Jebreen, H. Kanj. (2023). Topological Effects of Chiral Pamam Dendrimer for the Treatment of Cancer. Transylvanian Review. 31(2).

[39] H. Kanj, H. Iqbal, M.H. Aftab, H. Raza, K. Jebreen, M.I. Sowaity. (2023). Topological characterization of hexagonal network and non-kekulean benzenoid hydrocarbon. European Journal of Pure and Applied Mathematics. 16(4): 2187-2197.

[40] M.H. Aftab, A. Akgül, M.B. Riaz, M.A. Hussain, K. Jebreen, H. Kanj. (2024). Measuring the energy for the molecular graphs of antiviral agents: Hydroxychloroquine, Chloroquine and Remdesivir. South African Journal of Chemical Engineering. 47(1): 333-337.

[41] N. Ali, T. Khalifa, H. Iqbal, M.H. Aftab, K. Jebreen, H. Jamil, H. Kanj. (2024). Graphical Invariants for some Transformed Networks. European Journal of Pure and Applied Mathematics. 17(2): 690-709.